

Article

Bacillus velezensis TCS001 Enhances the Resistance of Hickory to *Phytophthora cinnamomi* and Reshapes the Rhizosphere Microbial Community

Chenshun Xie [†] , Yuntian Wu [†], Zhonghao Wu, Hao Cao , Xiaohui Huang, Feng Cui, Shuai Meng ^{*} and Jie Chen ^{*}

National Joint Local Engineering Laboratory for High-Efficient Preparation of Biopesticide, College of Forestry and Biotechnology, Zhejiang Agriculture and Forestry University, Hangzhou 311300, China; 13588373373@163.com (C.X.); wuyuntian0220@163.com (Y.W.); wzh12345@foxmail.com (Z.W.); ch990805hao@163.com (H.C.); 20173028@zafu.edu.cn (X.H.); cuifeng@zafu.edu.cn (F.C.)

^{*} Correspondence: mengshuai@zafu.edu.cn (S.M.); chenjie@zafu.edu.cn (J.C.)

[†] These authors contributed equally to this work.

Abstract: *Phytophthora cinnamomi* causes significant root rot in hickory, leading to substantial yield losses. While *Bacillus* spp. are recognized as beneficial rhizosphere microorganisms, their application against hickory root rot and their impact on rhizosphere microbial communities remain under-investigated. This study demonstrated that *Bacillus velezensis* TCS001 significantly inhibited *P. cinnamomi* ST402 growth in vitro, and achieved 71% efficacy in root rot disease management. Scanning electron microscopy (SEM) revealed that TCS001 fermentation filtrate induced mycelial deformities in *P. cinnamomi*. An analysis of α and β diversity indicated a significant impact of TCS001 on rhizosphere bacterial community richness and diversity, with minimal effects on the fungal community. Moreover, TCS001 altered the hickory rhizosphere microbiome co-occurrence network. The differential abundance analysis suggests that TCS001 promotes the recruitment of beneficial microbes associated with disease resistance, thereby suppressing disease development. These findings underscore the influence of TCS001 on the hickory rhizosphere microbiome in the presence of pathogens, providing valuable data for future research and the development of effective biocontrol strategies for hickory root rot.



Academic Editor: Nadia Massa

Received: 5 December 2024

Revised: 8 January 2025

Accepted: 13 January 2025

Published: 16 January 2025

Citation: Xie, C.; Wu, Y.; Wu, Z.; Cao, H.; Huang, X.; Cui, F.; Meng, S.; Chen, J. *Bacillus velezensis* TCS001 Enhances the Resistance of Hickory to *Phytophthora cinnamomi* and Reshapes the Rhizosphere Microbial Community. *Agriculture* **2025**, *15*, 193. <https://doi.org/10.3390/agriculture15020193>

Copyright: © 2025 by the authors. Licensee MDPI, Basel, Switzerland. This article is an open access article distributed under the terms and conditions of the Creative Commons Attribution (CC BY) license (<https://creativecommons.org/licenses/by/4.0/>).

Keywords: *Phytophthora cinnamomi*; *Bacillus velezensis* TCS001; *Carya cathayensis*; root rot; rhizosphere microbial

1. Introduction

Hickory (*Carya cathayensis*) is a common nutritional nut produced from a deciduous tree with feathered compound leaves and nuts, belonging to the *Juglandaceae* family, and it widely grows in the Zhejiang and Anhui provinces of China [1]. Currently, more than 15,000 ha of hickory are cultivated in Zhejiang Province, China, providing income to local farmers and conferring ecological protection in the mountainous areas of eastern China. However, traditional cultivation practices, such as monoculture, over-fertilization, and excessive herbicide application, have resulted in significant phytosanitary issues [2]. Recently, dieback disease caused by *Phytophthora cinnamomi* has posed a serious threat to hickory cultivation. A distinction was made between soilborne *Phytophthora* species, which primarily cause fine root losses, root and collar rots, and bleeding bark cankers, and airborne *Phytophthora* species, which are responsible for leaf necrosis, shoot blights, and fruit rot, as well as bleeding bark cankers, depending on whether their lifecycle occurs mainly above or below ground [3]. Dieback disease caused by *P. cinnamomi* broke out in

multiple orchards across Linan County, China's main production area [4]. The hickory leaves turn to yellow, wilt, and eventually fall off, leading to the death of the plants.

P. cinnamomi is a soil-borne pathogen whose life cycle consists of both sexual and asexual stages. It can grow saprophytically on dead organic matter and can also parasitize susceptible hosts. Typically, the pathogen infects fine lateral roots, but it can also invade woody stems, particularly through wounds or natural fractures in the epidermis. Growth within the root system can lead to root rot, disrupting water absorption and transport to the branches, resulting in wilting and yellowing of the leaves. Plants may die rapidly or survive for many years, but symptoms of the disease often do not appear. The ability of *P. cinnamomi* to grow saprophytically in soil or asymptotically in infected plants is a key factor in its long-term survival. The affected plants exhibited necrotic symptoms on the same side of the basal stem as the defoliated leaves, resulting in significant crop loss and severely impacting the income of local farmers and environmental safety.

The rhizosphere microbiome confers numerous benefits to plants, including enhanced nutrient acquisition, stress tolerance, and disease suppression [5,6]. Plant-associated microbes are increasingly recognized for their crucial role in disease resistance [7–9]. This influence is mediated through mechanisms such as microbial competition and antagonism toward pathogens [10–12], and the recruitment of beneficial microbes to enhance root colonization and mitigate pathogen attacks [13]. Growing interest in rhizosphere microbial communities reflects the increasing emphasis on ecological agriculture and sustainable development. Among beneficial bacteria, *Bacillus velezensis* has emerged as a key research subject due to its significant impact on plant health and disease resistance [14,15]. The robust spore-forming capability of *B. velezensis* ensures survival in diverse environments, while its production of various metabolites, including antibiotics and antifungal compounds, contributes to enhanced plant disease resistance [16,17]. Although the biocontrol potential and plant-growth-promoting effects of *Bacillus* spp. are well documented, the impact of *B. velezensis* on hickory dieback disease and its effects on the rhizosphere microbiome remain unexplored.

Microbial inoculants exert their influence not only directly on host plants, but also indirectly, by modulating the composition of the soil microbiome, thereby fostering the proliferation of advantageous microbes and contributing to disease suppression and growth enhancement. In this study, we verified the antifungal effect of *B. velezensis* TCS001 against the pathogen *Phytophthora cinnamomi* ST402 by treating hickory plants with TCS001. We also analyzed the impact of TCS001 on the microbial community in the rhizosphere of hickory through high-throughput sequencing of the rhizosphere soil, providing valuable insights for the future development of biocontrol agents against pathogens like *Phytophthora* in important forestry crops, such as hickory.

2. Materials and Methods

2.1. Plant Materials, Pathogen, and Soil Selection

Hickory seedlings were cultivated in a greenhouse with 24 °C day/night temperatures for 16 h/d with 80% relative humidity in the greenhouse. *Bacillus velezensis* TCS001 was isolated and identified in our laboratory (CGMCC No. 8921).

Phytophthora cinnamomi ST402 (obtained from Prof. Yongjun Wang, Zhejiang Agriculture and Forestry University), was used in this study. *Phytophthora cinnamomi* ST402 was cultured on V8 agar (3 g/L CaCO₃, 100 mL/L V8's 100% vegetable juice, 20 g/L agar) at 25 °C in the dark. Mycelial growth and phenotypic changes were assessed on V8 agar plates after seven days.

After streaking the strain *B. velezensis* TCS001 on LB agar and incubating for 48 h, a single colony was selected and inoculated into 80 mL of MLB seed medium (7 g/L peptone,

2 g/L yeast extract, 6 g/L NaCl, 2 g/L glucose, 0.06 g/L KCl, 0.5 g/L MgCl₂·6H₂O) and incubated at 27 °C and 145 rpm for 16 h. This seed culture was subsequently used as a 3% inoculum for a lipopeptide production medium (10.5 g/L soluble starch, 18.5 g/L peanut meal, 3 g/L NaCl, 32% *v/v*, pH 7.0), and incubated at 31 °C and 164 rpm for 48 h. The resulting fermentation broth was centrifuged (7830 rpm, 4 °C, 30 min) and then filter-sterilized (0.22 µm filter) four times using a sterile syringe and filter membrane to obtain the supernatant.

The supernatant was incorporated into molten potato dextrose agar (PDA) at a temperature range of 45–50 °C, achieving a final concentration of 20% (*v/v*). A mycelial plug, measuring 5 mm in diameter, from each pathogenic strain was positioned at the center of PDA plates containing the bacterial filtrate. These plates were then incubated at 25 °C for a period of five days. For comparison, control plates were prepared without the addition of the bacterial filtrate. Each experimental condition was replicated three times to ensure reliability. The inhibitory effect was quantified using the following formula: $y = (A - B)/A \times 100\%$ (A: growth radius of pathogen in control and B: growth radius of pathogen in different treatments).

To control for soil heterogeneity, a mixture of autoclaved nutrient substrate and air-dried soil (<4 mm) was used. Uniform *Carya* seedlings had their roots washed with sterile water before being transplanted into 0.5 L pots filled with sterilized soil substrate. One week post-transplantation, the control group (CK) received sterile water, while the treatment group (T6) received root irrigation with a *B. velezensis* TCS001 suspension (1×10^6 CFU/mL). The irrigation volume for both sterile water and TCS001 suspension was 200 mL. After a further week, both groups were inoculated with *P. cinnamomi*. The spore irrigation inoculation method was used to inoculate *Phytophthora cinnamomi*. *Phytophthora cinnamomi* V8 plates, cultured in the dark at 22 °C for 3–5 days, were soaked in 500 mL of ddH₂O. The water was replaced every 12 h to promote sporangium formation. Sterilized toothpicks were used to scrape the hyphae from the V8 medium containing sporangia into 500 mL of ddH₂O, which served as the irrigation solution. Each pot of hickory was inoculated by irrigating with 200 mL of the spore suspension. Disease Incidence = number of infected plants/total number of plants \times 100%.

The seedlings were cultivated in a greenhouse with regulated environmental parameters, including a temperature of 24 °C, a 16 h light cycle, and 80% relative humidity. They were irrigated using sterile double-distilled water (ddH₂O). The watering strategy was to maintain the surface soil of the pots in a moist condition. Rhizosphere soil samples were collected 45 days after inoculation with *Phytophthora cinnamomi*. Following the meticulous removal of surface soil, the plants were delicately uprooted. Any soil clinging to the roots was subsequently cleared using a sterilized brush. The rhizosphere soil samples were placed into 50 mL polypropylene tubes, rapidly frozen using liquid nitrogen, and then preserved at –80 °C. Each experimental condition included three biological replicates, with five plants pooled for each replicate (Figure 1).

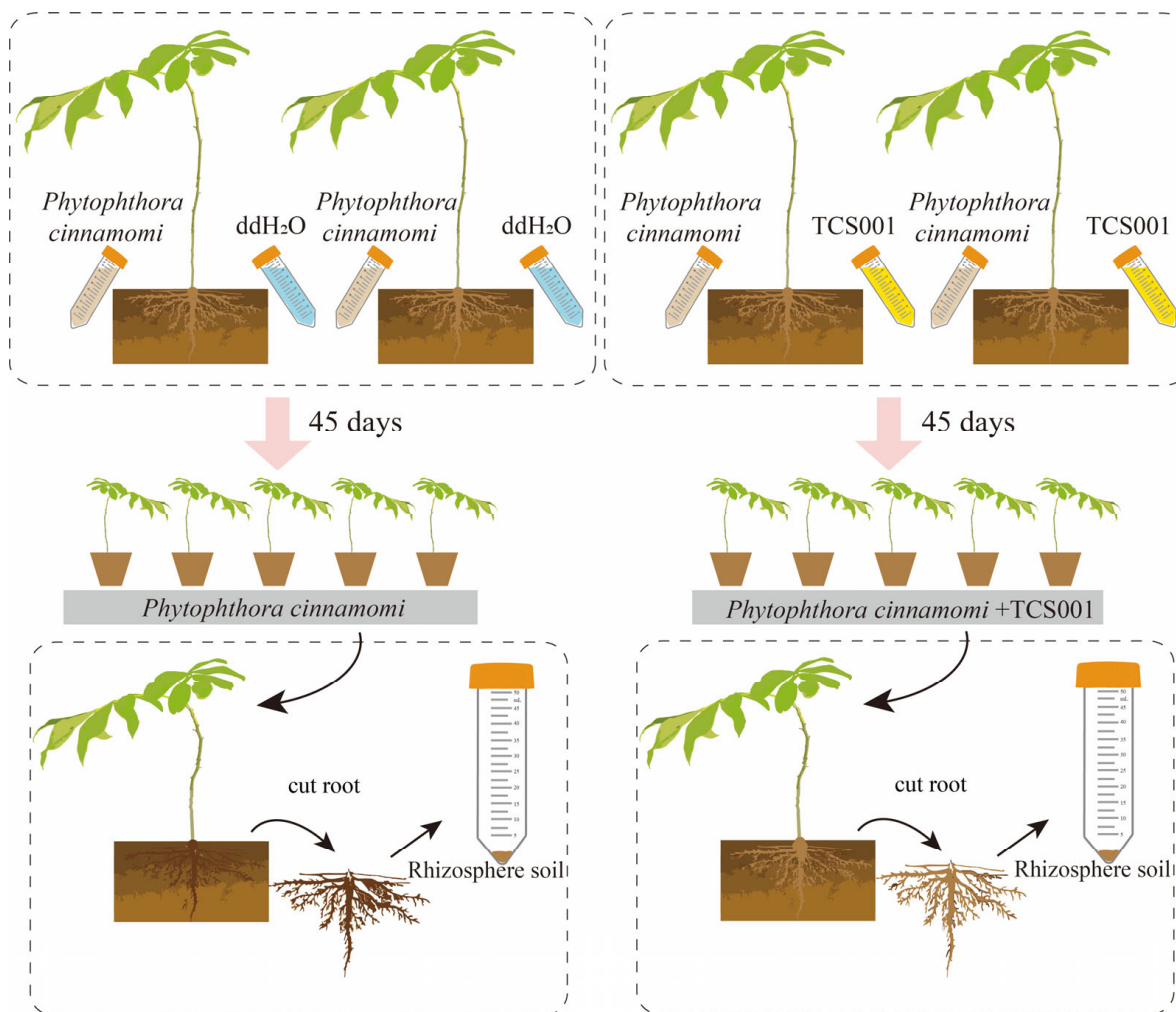


Figure 1. Schematic diagram. Control (CK) plants received sterile water irrigation, while treatment (T6) plants were irrigated with a *B. velezensis* TCS001 suspension. Seven days post-irrigation, both groups were root-inoculated with *P. cinnamomi* ST402. Rhizosphere soil was sampled for microbiome analysis 45 days post-inoculation.

2.2. DNA Extraction, PCR Amplification, and High-Throughput Sequencing

Genomic DNA was extracted from six soil samples using the E.Z.N.A.[®] Soil DNA Kit (Omega Bio-tek, Guangzhou, China), following the manufacturer's protocol. DNA quality and concentration were determined via 1% agarose gel electrophoresis and NanoDrop[®] ND-2000 spectrophotometry (Thermo Scientific, Wilmington, NC, USA) before storage at $-80\text{ }^{\circ}\text{C}$. Bacterial 16S rDNA and fungal ITS rDNA amplicons were generated using the primer pairs (5'-ACTCCTACGGGAGGCAGCAG-3') and 806R (5'-GGACTACHVGGGTWTCTAAT-3'), and for the ITS rDNA gene, the amplification was conducted with the primers ITS1-F (CTTGGTCATTTAGAGGAAGTAA) and ITS4-R (TCCTCCGCTTATTGATATGC), with an ABI GeneAmp[®] 9700 PCR thermocycler (Thermo Fisher Scientific, Eugene, OR USA). Each 20 μL PCR reaction contained 4 μL of 5 \times Fast Pfu buffer, 2 μL of 2.5 mM dNTPs, 0.8 μL of each primer (5 μM), 0.4 μL of Fast Pfu polymerase, 10 ng of template DNA, and ddH₂O. Thermal cycling conditions were as follows: 95 $^{\circ}\text{C}$ for 3 min, followed by 27 cycles of 95 $^{\circ}\text{C}$ for 30 s, 55 $^{\circ}\text{C}$ for 30 s, and 72 $^{\circ}\text{C}$ for 45 s, with a final extension at 72 $^{\circ}\text{C}$ for 10 min and a 4 $^{\circ}\text{C}$ hold. All samples were amplified in triplicate. PCR products were gel-extracted (2% agarose) using the AxyPrep DNA Gel Extraction Kit

(Axygen Biosciences, Hangzhou, China) and quantified using a Quantus™ Fluorometer (Promega, Beijing, China).

The purified amplicons were sequenced on the Illumina NovaSeq PE250 platform by Majorbio Bio-Pharm Technology Co. Ltd. (Shanghai, China) using standard protocols. Raw data were deposited in the NCBI Sequence Read Archive (SRA).

2.3. Data Processing and Bioinformatics Analysis

The raw FASTQ files were demultiplexed employing a custom Perl script developed in-house. Quality filtering and merging of paired-end reads were performed using fastp v0.19.6 and FLASH v1.2.7, respectively, applying the following criteria: (i) reads were trimmed at average quality scores <20 over a 50 bp sliding window, and those <50 bp were discarded, along with reads containing ambiguous bases; (ii) overlapping sequences ≥ 10 bp with a maximum mismatch ratio of 0.2 in the overlap region were merged; (iii) samples were demultiplexed based on barcode and primer sequences (exact barcode match, ≤ 2 nucleotide primer mismatches). Operational taxonomic units (OTUs) were derived from the analyzed sequences using UPARSE v7.1 [18,19], with a 97% sequence similarity threshold. The most frequently occurring sequence in each OTU was selected as its representative. To normalize sequencing depth, the 16S rRNA gene sequences were rarefied to 44,980 reads, and the ITS rDNA sequences to 84,995 reads, resulting in an average Good's coverage of 99.09%.

Taxonomic classification of OTU representative sequences was performed using RDP Classifier v2.2 against the SILVA database (v138.1 for bacteria) and UNITE database (v138.1 for fungi), with a confidence threshold of 0.7. The metagenome's functional potential was predicted using PICRUSt2 (Phylogenetic Investigation of Communities by Reconstruction of Unobserved States) [20]. The analysis utilized its integrated pipeline, which includes HMMER for sequence alignment, EPA-NG and Gappa for phylogenetic placement, castor for 16S gene copy normalization, and MinPath for predicting gene families and pathways. All steps adhered to the standard PICRUSt2 protocol.

Bioinformatic analysis of the soil microbiota was carried out using the Majorbio Cloud platform (<https://cloud.majorbio.com>). Based on the OTUs information, rarefaction curves and alpha diversity indices, including observed OTUs, Chao1 richness, Shannon index, and Good's coverage, were calculated with Mothur v1.30.1 [21]. The similarity among the microbial communities in different samples was determined by principal coordinate analysis (PCoA) based on Bray–Curtis dissimilarity using Vegan v2.5-3 package. The Welch *t*-test was used to calculate the significance of the differences between the two treatments using STAMP. The variations in the relative abundance of OTUs across different treatments were analyzed using likelihood ratio tests within the “EdgeR” package. A Manhattan plot was created utilizing the “ggplot2” package for visualization purposes.

2.4. Co-Occurrence Network Analysis

Co-occurrence networks for bacterial and fungal communities in control (CK) and treatment (T6) groups were constructed to investigate changes in microbial community interactions. Networks were generated using R (v4.3.1) based on Spearman correlation coefficients; only significant ($p < 0.05$) correlations with $|R| > 0.6$ were included [22]. Network visualization employed a Fruchterman–Reingold layout in Gephi.

2.5. Scanning Electron Microscopy (TEM) Observation

Fresh mycelia of *P. cinnamomi* ST402 on V8, treated with TCS001 fermentation filtrate, were collected and carefully fixed in 2.5% glutaraldehyde in phosphate buffer for at least 4 h. Samples were then processed and imaged via transmission electron microscopy (Hitachi H-7650) at Zhejiang University.

3. Results

3.1. The Biocontrol Effect of TCS001 on Hickory Diseases

Bacillus velezensis TCS001 and *Phytophthora cinnamomi* ST402 were used to assess biocontrol efficacy. A dual-culture assay demonstrated significant inhibition of *P. cinnamomi* ST402 growth by TCS001 (Figure 2A). Further, in planta experiments (Figure 1) showed that root irrigation with TCS001 (treatment T6) significantly reduced disease incidence (63%) in the presence of *P. cinnamomi* ST402, compared to the uninoculated control (CK), at over 86.5% (Figure 2B). The diseased leaves turn yellow and their roots rot, becoming black (Figure 2C). These findings demonstrated the effective biocontrol of *P. cinnamomi* ST402-induced hickory disease by TCS001 (Figure 2C,D and Figure S1).

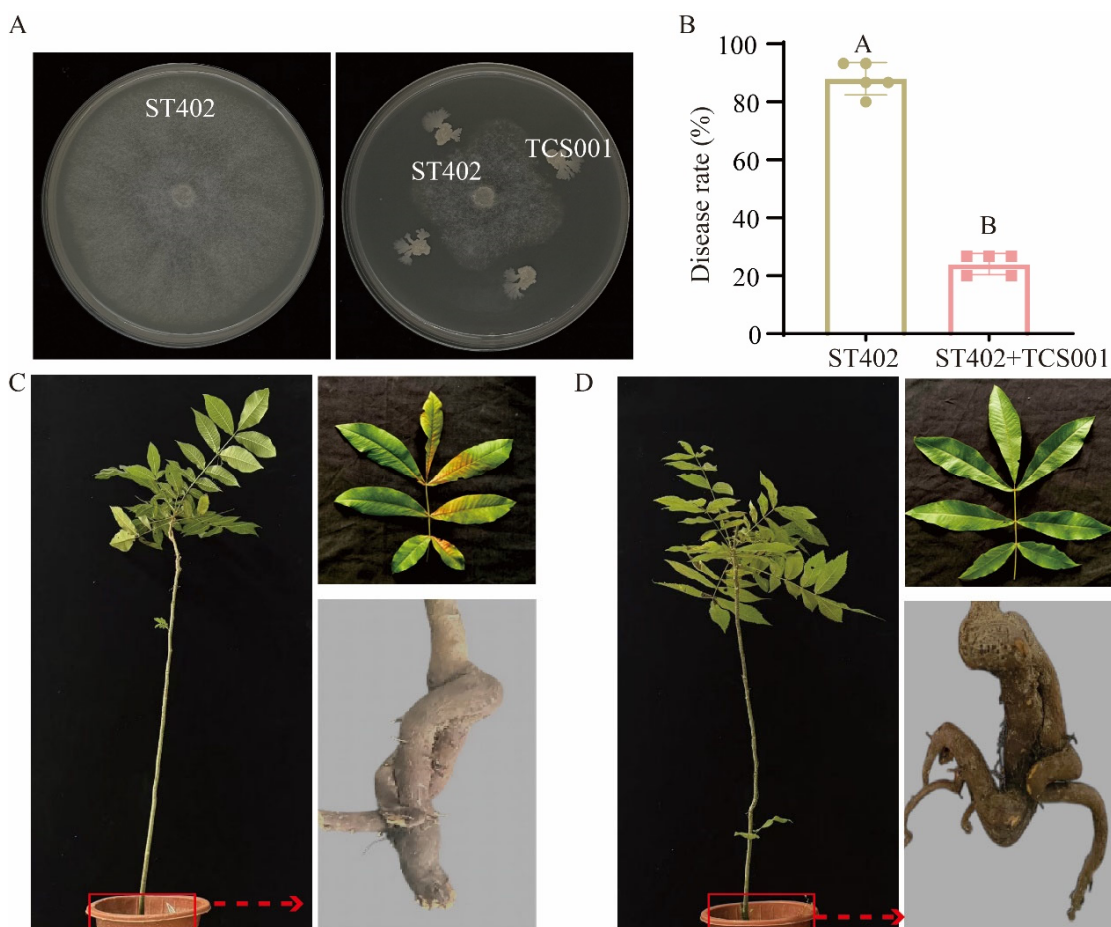


Figure 2. The biocontrol efficacy of *B. velezensis* TCS001 against *P. cinnamomi* ST402. (A) TCS001 inhibited the growth of *Phytophthora cinnamomi* ST402. (B) Disease rates for ST402 and ST402+TCS001. Growth performance of Hickory under different treatments. Different capital letters indicate significant differences between indices ($p < 0.01$, t -test). (C) The control group was inoculated with *Phytophthora cinnamomi* ST402 only. (D) The roots were irrigated with a bacterial solution of TCS001 and subsequently inoculated with *Phytophthora cinnamomi* ST402.

3.2. The Effect of TCS001 Fermentation Filtrate on the Growth of *Phytophthora Cinnamomi*

The antifungal activity of different concentrations of the TCS001 fermentation filtrate against *P. cinnamomi* ST402 was evaluated on a V8 medium (Figure 3A). As shown in Figure 3, different concentrations of fermentation filtrate have varying inhibitory effects on the pathogen *P. cinnamomi* ST402, with values of 68%, 49%, and 36%, respectively (Figure 3B). Additionally, the optimal treatment condition for the TCS001 fermentation filtrate was determined to be a liquid-to-water dilution ratio of 1:5. The results indicated that TCS001 fermentation filtrate can inhibit the development growth of *Phytophthora cinnamomi*.

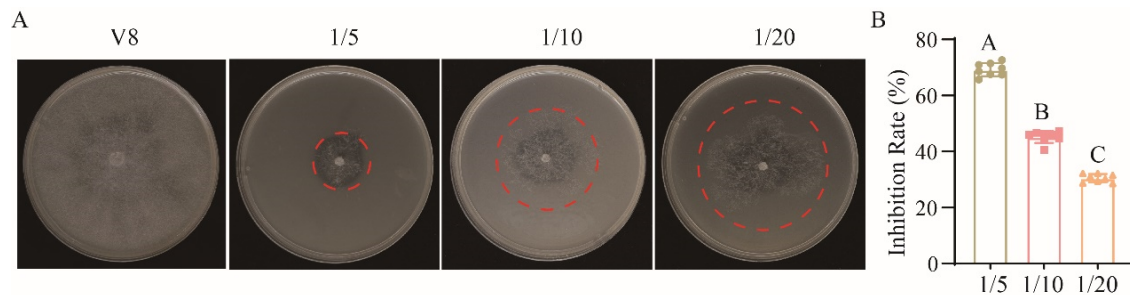


Figure 3. The assay for the inhibitory activity against *Phytophthora cinnamomi* ST402. (A) The in vitro antifungal activity of TCS001 fermentation filtrate was evaluated at serial dilution ratios of 1/5, 1/10, and 1/20 (fermentation filtrate to medium). (B) Inhibition rates were calculated for Petri dishes treated with TCS001 fermentation filtrate at the specified dilutions. Significant differences between indices are indicated by distinct capital letters ($p < 0.01$, t -test).

3.3. Scanning Electron Microscopy (SEM) Observation of Hyphae Cultured on a Medium Diluted Fivefold with Fermentation Filtrate

Scanning electron microscopy (SEM) was used to examine *P. cinnamomi* ST402 hyphae grown on a V8 medium containing a fivefold dilution of TCS001 fermentation filtrate. The control hyphae exhibited smooth surfaces (Figure 4A), while the hyphae treated with TCS001 filtrate showed breakage, twisting, and deformation (Figure 4B). These findings indicated that the TCS001 fermentation filtrate altered the *P. cinnamomi* ST402 hyphal morphology.

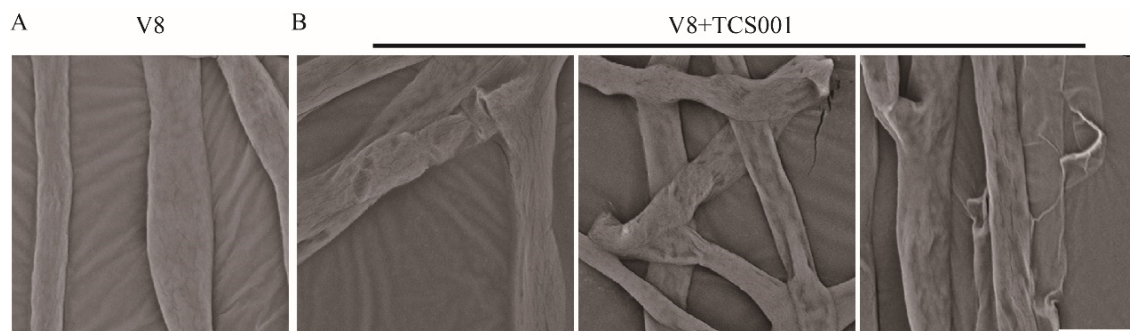


Figure 4. Morphological changes of *P. cinnamomi* mycelia grown on V8 amended with fermentation filtrate of TCS001. (A) control; (B) treatment group.

3.4. Characterization of Amplicon Sequencing Datasets

To examine the influence of *B. velezensis* TCS001 on the hickory rhizosphere microbiome, high-throughput sequencing was conducted on six rhizosphere soil samples. Rarefaction curves for both 16S rRNA and ITS gene amplicons indicated sufficient sequencing depth to capture community diversity (Figure S1). A total of 379,897 high-quality 16S rRNA sequences (59,430–69,804 per sample; average length 412.40 bp) and 559,998 high-quality ITS sequences (85,193–97,923 per sample; average length 241.52 bp) were obtained (Table S1). Taxonomic assignment was performed using SILVA (bacteria) and UNITE (fungi) databases with a 97% similarity threshold, employing a Bayesian classifier and BLAST. This resulted in 1283 bacterial and 522 fungal OTUs, representing 35 bacterial and 15 fungal phyla, respectively. A further analysis focused on OTUs with a relative abundance $>0.05\%$, yielding 401 bacterial and 474 fungal OTUs. These data were used to assess the effects of TCS001 on the hickory rhizosphere microbiome.

3.5. CK and T6 Have Significantly Different Rhizosphere Microbial Communities

To characterize the effects of TCS001 on the changes in the rhizosphere microbial communities of hickory after inoculation with pathogenic fungi *P. cinnamomi*, the α diversity of the fungal and bacterial communities was analyzed using the Chao1 index and Shannon index. Our analyses showed that after inoculation with *P. cinnamomi*, TCS001 had a significant impact on the diversity and richness of the hickory bacterial community ($p < 0.05$), but it did not have a significant effect on the fungal community (Figures 5 and 6). The bacterial Chao1 index and Shannon index in the CK were significantly higher than those in the rhizosphere soil treated with TCS001 ($p < 0.05$) (Figure 5A,B). For the fungal community, the Chao index of the CK group rhizosphere soil was lower than that of the T6 group, while the Shannon index showed the opposite trend, although this change was not significant ($p > 0.05$) (Figure 6A). Furthermore, a principal coordinate analysis (PCoA) based on Bray–Curtis distance further revealed significant differences in the rhizosphere microbial communities of hickory due to TCS001 (Figure 6B). We found that samples inoculated with pathogenic fungi *P. cinnamomi* could be distinguished from those inoculated with the pathogenic fungi *P. cinnamomi* and TCS001 in bacterial communities (Figure 5C), while in fungal communities, the six samples clustered together and could not be distinguished (Figure 6C). This result, combined with the Chao and Shannon index results, indicated that TCS001 significantly affects the composition of the rhizosphere bacterial community.

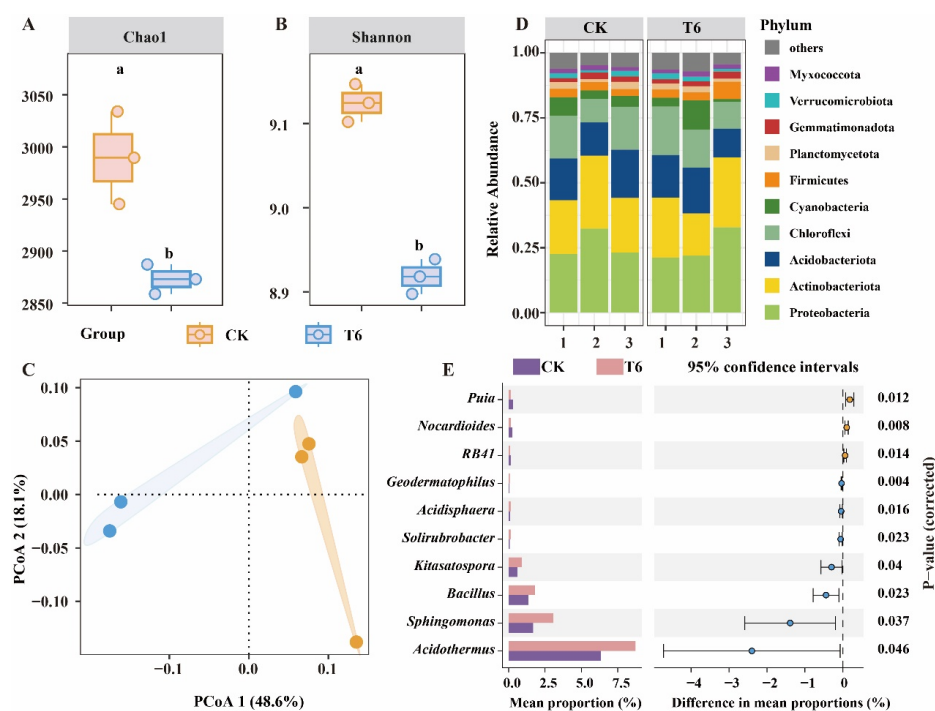


Figure 5. Analysis of bacterial alpha and beta diversity, as well as microbiome composition. Alpha diversity, assessed using the Chao (A) and Shannon (B) indices, demonstrated variation among rhizosphere soil samples across different treatments, with significant differences denoted by distinct lowercase letters ($p < 0.05$, Tukey test). Principal coordinate analysis (PCoA) based on the Bray–Curtis distance matrix (C) revealed distinct clustering patterns. The relative abundance of bacterial phyla in rhizosphere soil samples from treated plants is displayed in (D). Significant differences in bacterial phyla levels were identified using the Kruskal–Wallis H test (E). (Lowercase letters indicate significant differences).

We further assessed the relative abundance of bacteria at both the phylum and genus levels. The composition of the bacterial community was examined at these taxonomic levels. Proteobacteria, Actinobacteriota, and Acidobacteriota were the dominant phyla in both control (CK) and treatment (T6) groups (Figure 5D; Table S2), with similar relative

abundances, as follows: *Proteobacteria* (CK: 26.04%; T6: 25.36%), *Actinobacteriota* (CK: 23.28%; T6: 22.12%), and *Acidobacteriota* (CK: 15.81%; T6: 14.98%). At the genus level, the Welch's *t* test revealed significant differences ($p < 0.05$) in the relative abundance of ten genera between CK and T6 (Figure 5E). Seven genera showed significantly increased abundance in T6 compared to CK (Figure 5E), including *Acidotherrmus*, *Sphingomonas*, and *Bacillus* (increases of 2.40%, 1.39%, and 0.45%, respectively; Table S2).

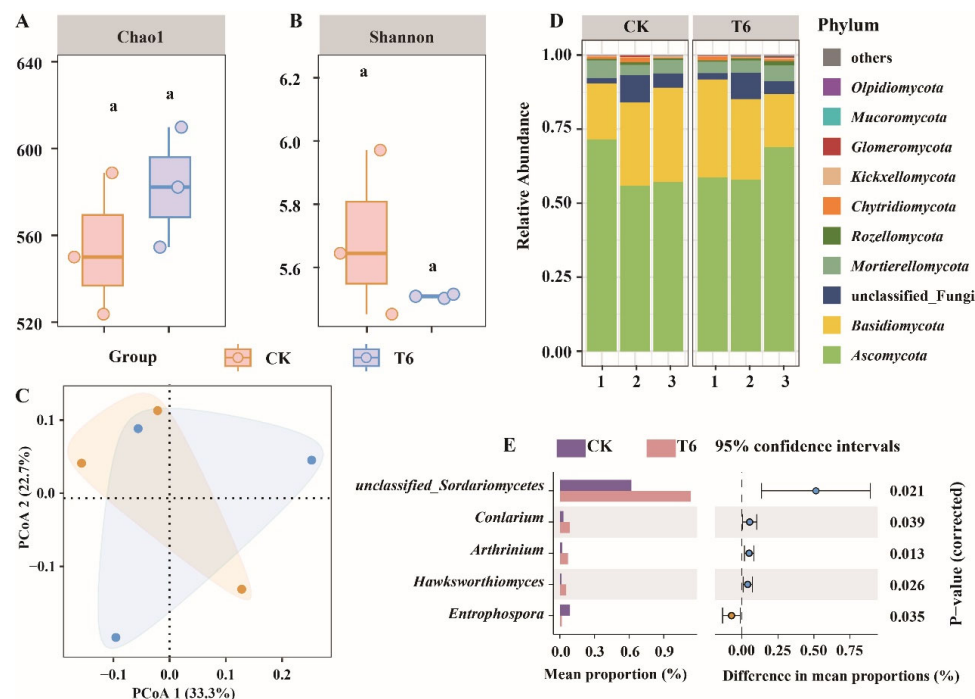


Figure 6. Fungal diversity and microbiome composition were analyzed across different rhizosphere soil samples. Fungal alpha diversity, evaluated using the Chao (A) and Shannon (B) indices, showed significant variation across treatments, with distinct lowercase letters marking significant differences ($p < 0.05$, Tukey test). Principal coordinate analysis (PCoA) based on the Bray–Curtis distance matrix (C) demonstrated distinct clustering patterns. The relative abundances of fungal phyla in rhizosphere soil samples from different treatments are displayed in (D). The Kruskal–Wallis H test (E) revealed significant differences in fungal phyla. (Lowercase letters indicate significant differences).

In the fungal community, Ascomycota and Basidiomycota were the dominant phyla in both control (CK) and treatment (T6) groups (Figure 6D; Table S2), with similar relative abundances, as follows: Ascomycota (CK: 61.52%; T6: 61.89%) and Basidiomycota (CK: 26.30%; T6: 26.10%). While *Ascomycota* showed a slightly higher relative abundance in T6, this difference was not statistically significant ($p > 0.05$). At the genus level, five fungal genera showed significant differences between CK and T6 (Figure 6E). *Unclassified Sor-dariomycetes*, *Conlarium*, *Arthrinium*, and *Hawksworthiomyces* exhibited significantly higher relative abundances in CK (increases of 0.47%, 0.02%, 0.08%, and 0.04%, respectively; Figure 6E; Table S2), while *Entrophospora* showed a significantly higher relative abundance in T6 (0.02% increase). These results indicate that TCS001 modifies the structure of bacterial and fungal communities within the hickory rhizosphere.

3.6. Specific Differences in Rhizosphere Soil Microbiomes

To further characterize microbial community shifts, we compared the OTU abundance between the control (CK; pathogen-inoculated) and treatment (T6; pathogen and TCS001-inoculated) hickory rhizosphere samples using Manhattan and scatter plots. Significantly differentially abundant OTU values were identified ($p < 0.05$; Figure 7A,B; Tables S4 and S5): 144 bacterial OTUs and 81 fungal OTUs. These belonged to 20 bacterial phyla (Table

S3), with *Proteobacteria* (33 OTUs), *Chloroflexi* (25 OTUs), and *Acidobacteriota* (15 OTUs) showing the most significant differences. The 81 differentially abundant fungal OTUs represented six known phyla and one unclassified phylum (Table S3), with *Ascomycota* (39 OTUs), *Basidiomycota* (17 OTUs), and unclassified fungi (16 OTUs) exhibiting the greatest differences (Table S4). T6 showed enrichment of 72 bacterial and 48 fungal OTUs compared to the CK (Tables S3 and S4), while the top 10 differentially abundant OTUs included more fungi than bacteria (32 vs. 16; Figure 7C,D), suggesting that bacteria may harbor more low-abundance differentially abundant OTUs. Notably, the potential pathogen *Aspergillus* (OTU1300) was significantly less abundant in T6 (Table S4), while beneficial bacteria such as *Sphingomonas* (OTU3182) and *Bacillus* (OTU2812) were enriched in T6 (Table S3). These results indicate that co-inoculation with TCS001 promotes the recruitment of beneficial microbes in the rhizosphere in response to pathogen challenge.

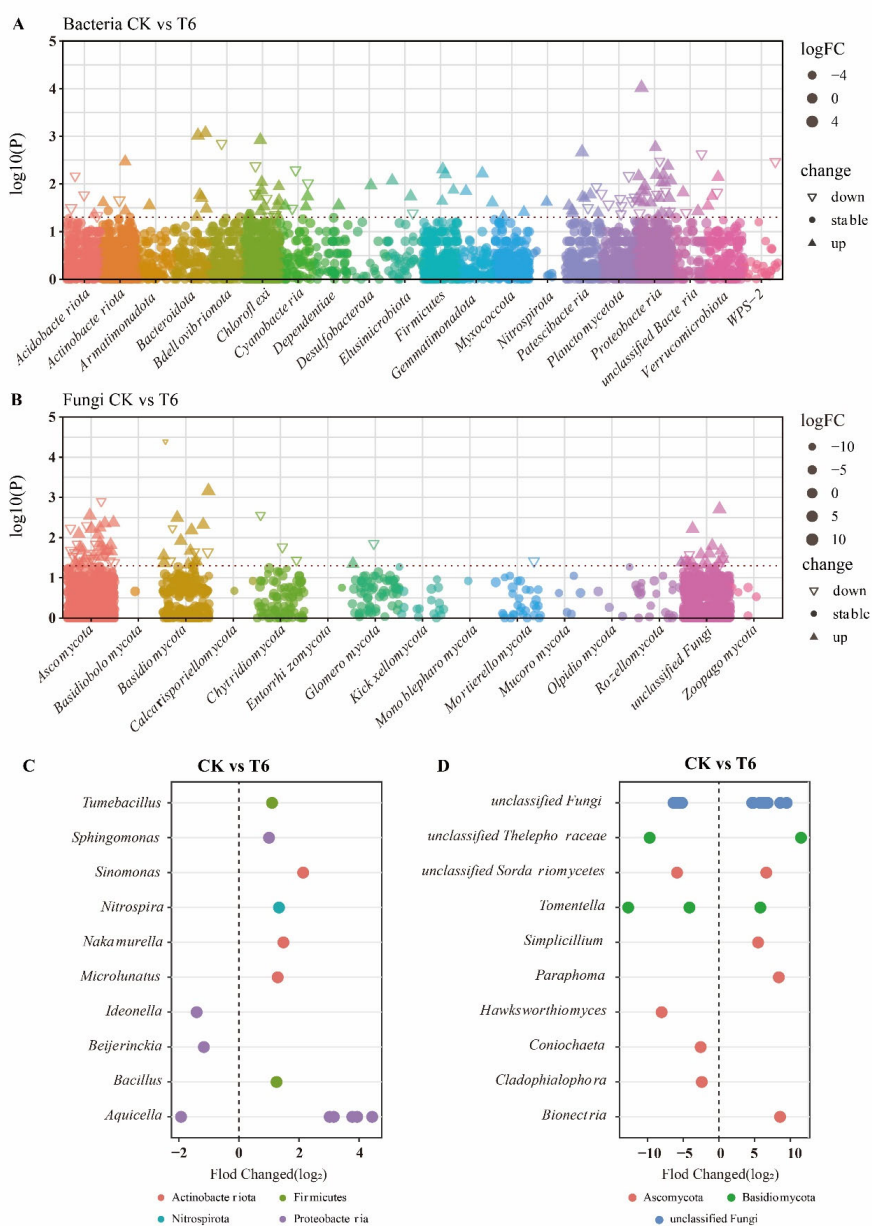


Figure 7. Enrichment (up) and depletion (down) of bacterial (A) and fungal (B) OTUs between CK and T6 groups. Comparative analysis of the top 10 bacterial (C) and fungal (D) genera showing significant enrichment or depletion in OTUs between CK and T6 treatment groups. Colors of points indicate phylum classification.

3.7. Characterization of the Rhizosphere Microbiome Co-Occurrence Networks

To investigate the effect of TCS001 on hickory rhizosphere microbial co-occurrence networks, bacterial and fungal networks were constructed (Figure 8). We analyzed the proportion of the fungal and bacterial network graphs at the phylum level. In the bacterial co-occurrence network, compared with CK, the proportions of Actinobacteriota, Chloroflexi, Gemmatimonadota, Firmicutes, Myxococcota, and WPS-2 increased in the T6 group. Similarly, in the fungal network, after inoculating TCS001, the proportion of five fungal phyla (unclassified fungi, Chytridiomycota, Kickxellomycota, Rozellomycota, and Glomeromycota) increased, and the ranking of eight bacterial phyla and seven fungal phyla also underwent changes (Figure 8A,C, Table S5).

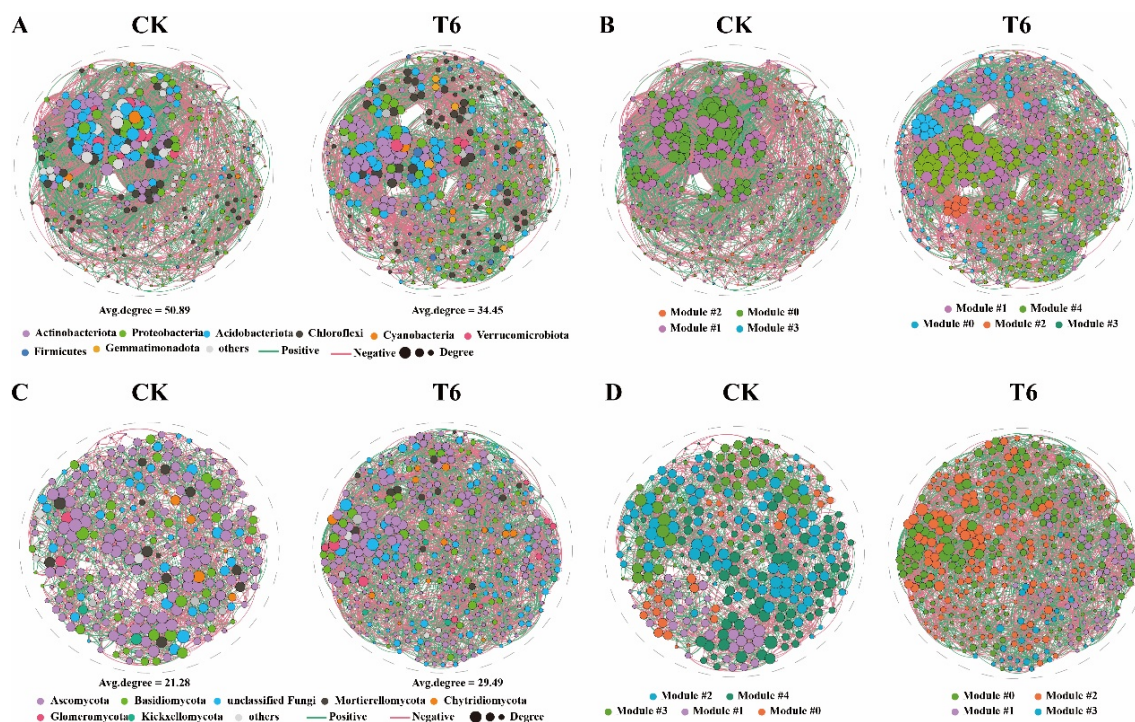


Figure 8. Bacterial and fungal co-occurrence networks. The bacterial (A,B) and fungal (C,D) co-occurrence networks were constructed using the Spearman correlation coefficient at the OTU level, displaying connections that represent statistically significant correlations ($p < 0.05$) with magnitudes > 0.6 (positive correlation—blue edges) or < -0.6 (negative correlation—purple edges). Distinct colors correspond to different phyla (A,C) and module classes (B,D).

We also analyzed the topology of the co-occurrence networks. The control (CK) bacterial network comprised 377 nodes and 9440 edges, while the fungal network comprised 299 nodes and 3182 edges (Table S6). Following TCS001 inoculation (T6), the bacterial network had 367 nodes and 6371 edges, and the fungal network had 437 nodes and 6444 edges (Table S6). These changes suggest stronger connectivity within the CK bacterial network compared to the T6 bacterial network, and the opposite trend for the fungal networks. The T6 bacterial network displayed a higher proportion of positive edges (CK: 52.87%; T6: 56.34%) and the T6 fungal network exhibited a higher average degree (CK: 21.28; T6: 29.49; Figure 8C, Table S6). Both bacterial and fungal networks showed reduced density following TCS001 inoculation (bacterial: CK 0.138, T6 0.094; fungal: CK 0.071, T6 0.068; Table S6). We also found that after inoculation with the antagonistic bacterium TCS001, the modularity of the bacterial network became more concentrated. In the bacterial network, the CK group had five modules, the T6 group had four modules, and the fungal network was exactly the

opposite of the bacterial network (Figure 8B,D). These findings demonstrate that TCS001 application alters the structure of the rhizosphere microbial network.

4. Discussion

Members of the genus *Bacillus* are widely recognized for their potential as biocontrol agents due to their robust growth, stable physicochemical properties, and broad antimicrobial spectrum [23]. Numerous studies have demonstrated the plant-growth-promoting and disease-suppressing capabilities of various *Bacillus* strains, highlighting their versatility in different agricultural systems. For instance, *Bacillus amyloliquefaciens* FZB42 and FZB24 have been extensively studied for their ability to suppress diseases in potatoes [24], cotton [25], strawberries [26], wheat [27], lettuce [28], and tomatoes [29]. These strains produce a variety of secondary metabolites, including lipopeptides and polyketides, which exhibit strong antifungal and antibacterial activities, thereby protecting plants from soil-borne pathogens [16,17]. Similarly, *Bacillus velezensis* AP-3 has been shown to enhance salt stress tolerance in tomatoes by modulating the plant's antioxidant defense system and improving nutrient uptake [30]. In another study, *Bacillus velezensis* K-9 demonstrated significant efficacy against potato scab, a disease caused by *Streptomyces scabies*, by producing antimicrobial compounds that inhibit pathogen growth [31]. Furthermore, *Bacillus velezensis* VJH504 has been reported to control cucumber Fusarium wilting by inducing systemic resistance in the plant and altering the rhizosphere microbiome to favor beneficial microbes [23]. This study further demonstrates the efficacy of *Bacillus velezensis* TCS001 against *Phytophthora cinnamomi*, the causal agent of hickory root rot, through both plate confrontation and pot experiments. The findings align with previous research on *Bacillus* species, reinforcing their potential as biocontrol agents in diverse agricultural systems.

Phytophthora cinnamomi infection primarily occurs via the active movement of biflagellate zoospores, although mycelial growth also contributes to disease spread [32]. Zoospores are chemotactically attracted to the root elongation zone, preferentially settling in grooves above anticlinal epidermal cell walls. At high densities, zoospores exhibit self-aggregation and clustering, influenced by chemotaxis and bioconvection. Attachment to the root surface is mediated by the 250 kDa adhesive protein PcVsv1 [33], secreted from ventral vesicles. Subsequent penetration and colonization involve the action of various plant-cell-wall-degrading enzymes [34]. Following attachment, mycelial growth proceeds through the root cortex, both inter- and intracellularly, ultimately reaching the vascular bundle. Xylem blockage by the mycelium disrupts water transport, leading to water stress and plant death.

Bacillus species offer a promising biocontrol strategy by interfering with multiple stages of *Phytophthora* infection [10,11]. Studies have shown that *Bacillus amyloliquefaciens* can inhibit *Phytophthora* zoospore germination and motility, limiting their ability to infect host plants [12]. In this study, *Bacillus velezensis* TCS001 likely disrupts *P. cinnamomi* infection by producing antifungal metabolites that inhibit zoospore germination and hyphal growth, as evidenced by SEM observations of deformed hyphae. TCS001 may also enhance the plant's innate immune response, reducing susceptibility to *P. cinnamomi* infection, aligning with previous research on *Bacillus* species' ability to combat soilborne pathogens.

Microbial inoculants, including *Bacillus* spp., can enhance beneficial rhizosphere microbial communities, such as *Flavobacterium*, *Pseudomonas*, *Agrobacterium*, and *Lysobacter*, while suppressing soilborne pathogens [13,35]. *Bacillus* spp. promote rhizobial colonization, enhance the abundance of *Flavobacterium johnsoniae*, and stimulate local *Pseudomonas* populations, contributing to disease suppression [36–38]. For example, *B. velezensis* SQR9 increases the relative abundance of *Pseudomonas*, *Bacillus*, and *Lysobacter*, synergistically promoting plant growth with native *Pseudomonas stutzeri* [39]. This study shows that TCS001 application increases the relative abundance of *Sphingomonas*, a genus consistently enriched

in healthy plants, including ginger [40] and disease-resistant tomatoes [41]. In rice, *Sphingomonas melonis* enhances resistance to *Burkholderia plantarii* [42]. These findings suggest that TCS001 may suppress *P. cinnamomi* infection by promoting *Sphingomonas* enrichment in the rhizosphere. Additionally, recent research has demonstrated that *Bacillus*-mediated changes in the rhizosphere microbiome can lead to long-term disease suppression by enhancing the abundance of antagonistic microbes and improving plant immune responses [39,43].

The fungal community in the hickory rhizosphere showed minimal changes in response to *Bacillus velezensis* TCS001 treatment. Certain fungal taxa, such as *Aspergillus*, exhibited reduced abundance in the TCS001-treated rhizosphere, indicating that TCS001 may indirectly suppress some fungal pathogens by promoting beneficial bacteria that compete with or antagonize these fungi [40,41]. Additionally, the increased connectivity and modularity of the bacterial co-occurrence network in TCS001-treated soils may create a more resilient microbial environment that limits the establishment of fungal pathogens [44,45]. While the overall fungal community remained relatively stable, the specific reduction in potential fungal pathogens suggests that TCS001 could still play a role in managing fungal diseases, albeit indirectly, through its impact on the rhizosphere microbiome. Recent studies have highlighted the critical role of microbial modulations in plant stress responses, particularly under conditions such as drought, salinity, and pathogen attack [46–48].

This study investigated the impact of *B. velezensis* TCS001 on the structure of bacterial and fungal co-occurrence networks in the hickory rhizosphere to elucidate its mechanism of action against environmental perturbations. Meanwhile, the inhibitory effect of TCS001 fermentation products on *P. cinnamomi* suggests their potential as a biocontrol agent for hickory root rot. Higher average degree and network density indicate increased sensitivity to environmental change, while high connectivity provides functional redundancy [49]. Network effectiveness was assessed using average degree and network density [43] by comparing co-occurrence networks with and without TCS001 inoculation. The bacterial community exhibited higher average degree and network density than the fungal community, particularly before inoculation, indicating a more robust network structure. This aligns with previous findings, such as the disease-suppressing effects of *B. velezensis* ZN-510 against tomato bacterial necrosis [50], highlighting the importance of antagonistic bacteria in shaping soil microbial community structure. The increased bacterial connectivity provides functional redundancy, enhancing resilience to pathogen infection. TCS001 inoculation thus altered the rhizosphere microbial network structure and enhanced disease resistance, offering valuable insights for future research.

5. Conclusions

In summary, our study suggests that TCS001 enhances the recruitment of beneficial microbes associated with disease resistance, thereby inhibiting disease development. These results highlight that TCS001 restructures the rhizosphere microbial community in the presence of *P. cinnamomi*, offering critical insights for future studies and the advancement of effective biocontrol approaches to combat hickory root rot.

Supplementary Materials: The following supporting information can be downloaded at <https://www.mdpi.com/article/10.3390/agriculture15020193/s1>. Figure S1 Disease incidence of hickory inoculated with the isolated pathogen. Hickory. (A) without treatment.; (B) inoculated with *Phytophthora cinnamomi*. Figure S2 Rarefaction curves of 6 samples for 16S rDNA gene sequencing (A) and ITS gene sequencing (B). Table S1. Summary on raw data process. Table S2. The relative abundance of bacterial communities at the phylum level. Table S3. Differential abundance of bacterial OTUs between CK and T6. Table S4. Differential abundance of fungal OTUs between CK and T6. Table S5. The Proportions of Phylum in fungal network. Table S6. Topology properties of the networks.

Author Contributions: S.M. and J.C. planned and designed the research. Z.W., H.C., X.H. and F.C. performed the experiments and analyzed the data. C.X. and Y.W. wrote the manuscript. All authors have read and agreed to the published version of the manuscript.

Funding: This research was supported by the National Key Research and Development Program of China (2022YFD1700400).

Institutional Review Board Statement: Not applicable.

Data Availability Statement: The original contributions presented in this study are included in the article.

Conflicts of Interest: The authors declare no conflict of interest.

References

1. Yang, J.; Zhou, F.; Xiong, L.; Mao, S.; Hu, Y.; Lu, B. Comparison of phenolic compounds, tocopherols, phytosterols and antioxidant potential in Zhejiang pecan [*Carya cathayensis*] at different stir-frying steps. *LWT—Food Sci. Technol.* **2015**, *62*, 541–548. [[CrossRef](#)]
2. Morales-Rodríguez, C.; Wang, Y.; Martignoni, D.; Vannini, A. *Phytophthora cathayensis* sp. nov., a new species pathogenic to Chinese Hickory (*Carya cathayensis*) in southeast China. *Fungal Syst. Evol.* **2020**, *7*, 99–111. [[CrossRef](#)]
3. Davison, E.M. *Phytophthora* Diseases Worldwide. *Plant Pathology* **1998**, *47*, 224–225. [[CrossRef](#)]
4. Tong, X.; Wu, J.; Mei, L.; Wang, Y. Detecting *Phytophthora cinnamomi* associated with dieback disease on *Carya cathayensis* using loop-mediated isothermal amplification. *PLoS ONE* **2021**, *16*, e0257785. [[CrossRef](#)]
5. Mendes, R.; Kruijt, M.; de Bruijn, I.; Dekkers, E.; van der Voort, M.; Schneider, J.H.M.; Piceno, Y.M.; DeSantis, T.Z.; Andersen, G.L.; Bakker, P.A.H.M.; et al. Deciphering the Rhizosphere Microbiome for Disease-Suppressive Bacteria. *Science* **2011**, *332*, 1097–1100. [[CrossRef](#)]
6. Liu, H.; Brettell, L.E.; Qiu, Z.; Singh, B.K. Microbiome-Mediated Stress Resistance in Plants. *Trends Plant Sci.* **2020**, *25*, 733–743. [[CrossRef](#)]
7. Kwak, M.-J.; Kong, H.G.; Choi, K.; Kwon, S.-K.; Song, J.Y.; Lee, J.; Lee, P.A.; Choi, S.Y.; Seo, M.; Lee, H.J.; et al. Rhizosphere microbiome structure alters to enable wilt resistance in tomato. *Nat. Biotechnol.* **2018**, *36*, 1100–1109. [[CrossRef](#)]
8. Castrillo, G.; Teixeira, P.J.P.L.; Paredes, S.H.; Law, T.F.; de Lorenzo, L.; Feltcher, M.E.; Finkel, O.M.; Breakfield, N.W.; Mieczkowski, P.; Jones, C.D.; et al. Root microbiota drive direct integration of phosphate stress and immunity. *Nature* **2017**, *543*, 513–518. [[CrossRef](#)]
9. Berendsen, R.L.; Vismans, G.; Yu, K.; Song, Y.; de Jonge, R.; Burgman, W.P.; Burmølle, M.; Herschend, J.; Bakker, P.A.H.M.; Pieterse, C.M.J. Disease-induced assemblage of a plant-beneficial bacterial consortium. *ISME J.* **2018**, *12*, 1496–1507. [[CrossRef](#)]
10. Yin, X.-T.; Xu, L.; Fan, S.-S.; Xu, L.-N.; Li, D.-C.; Liu, Z.-Y. Isolation and characterization of an AHL lactonase gene from *Bacillus amyloliquefaciens*. *World J. Microbiol. Biotechnol.* **2010**, *26*, 1361–1367. [[CrossRef](#)]
11. Pane, C.; Zaccardelli, M. Evaluation of *Bacillus* strains isolated from solanaceous phylloplane for biocontrol of *Alternaria* early blight of tomato. *Biol. Control* **2015**, *84*, 11–18. [[CrossRef](#)]
12. Dimopoulou, A.; Theologidis, I.; Liebmann, B.; Kalantidis, K.; Vassilakos, N.; Skandalis, N. *Bacillus amyloliquefaciens* MBI600 differentially induces tomato defense signaling pathways depending on plant part and dose of application. *Sci. Rep.* **2019**, *9*, 19120. [[CrossRef](#)] [[PubMed](#)]
13. Qin, Y.; Shang, Q.; Zhang, Y.; Li, P.; Chai, Y. *Bacillus amyloliquefaciens* L-S60 Reforms the Rhizosphere Bacterial Community and Improves Growth Conditions in Cucumber Plug Seedling. *Front. Microbiol.* **2017**, *8*, 2620. [[CrossRef](#)]
14. Choudhary, D.K.; Johri, B.N. Interactions of *Bacillus* spp. and plants—With special reference to induced systemic resistance (ISR). *Microbiol. Res.* **2009**, *164*, 493–513. [[CrossRef](#)] [[PubMed](#)]
15. Chen, Y.; Li, Y.; Fu, Y.; Jia, L.; Li, L.; Xu, Z.; Zhang, N.; Liu, Y.; Fan, X.; Xuan, W.; et al. The beneficial rhizobacterium *Bacillus velezensis* SQR9 regulates plant nitrogen uptake via an endogenous signaling pathway. *J. Exp. Bot.* **2024**, *75*, 3388–3400. [[CrossRef](#)] [[PubMed](#)]
16. Chen, X.H.; Koumoutsis, A.; Scholz, R.; Eisenreich, A.; Schneider, K.; Heinemeyer, I.; Morgenstern, B.; Voss, B.; Hess, W.R.; Reva, O.; et al. Comparative analysis of the complete genome sequence of the plant growth-promoting bacterium *Bacillus amyloliquefaciens* FZB42. *Nat. Biotechnol.* **2007**, *25*, 1007–1014. [[CrossRef](#)] [[PubMed](#)]
17. Ongena, M.; Jacques, P. *Bacillus* lipopeptides: Versatile weapons for plant disease biocontrol. *Trends Microbiol.* **2008**, *16*, 115–125. [[CrossRef](#)]
18. Edgar, R.C. UPARSE: Highly accurate OTU sequences from microbial amplicon reads. *Nat. Methods* **2013**, *10*, 996–998. [[CrossRef](#)]
19. Stackebrandt, E.; Goebel, B.M. Taxonomic Note: A Place for DNA-DNA Reassociation and 16S rRNA Sequence Analysis in the Present Species Definition in Bacteriology. *Int. J. Syst. Evol. Microbiol.* **1994**, *44*, 846–849. [[CrossRef](#)]

20. Douglas, G.M.; Maffei, V.J.; Zaneveld, J.R.; Yurgel, S.N.; Brown, J.R.; Taylor, C.M.; Huttenhower, C.; Langille, M.G.I. PICRUSt2 for prediction of metagenome functions. *Nat. Biotechnol.* **2020**, *38*, 685–688. [[CrossRef](#)]
21. Schloss Patrick, D.; Westcott Sarah, L.; Ryabin, T.; Hall Justine, R.; Hartmann, M.; Hollister Emily, B.; Lesniewski Ryan, A.; Oakley Brian, B.; Parks Donovan, H.; Robinson Courtney, J.; et al. Introducing mothur: Open-Source, Platform-Independent, Community-Supported Software for Describing and Comparing Microbial Communities. *Appl. Environ. Microbiol.* **2009**, *75*, 7537–7541. [[CrossRef](#)] [[PubMed](#)]
22. Barberán, A.; Bates, S.T.; Casamayor, E.O.; Fierer, N. Using network analysis to explore co-occurrence patterns in soil microbial communities. *ISME J.* **2012**, *6*, 343–351. [[CrossRef](#)] [[PubMed](#)]
23. Yang, F.; Jiang, H.; Ma, K.; Wang, X.; Liang, S.; Cai, Y.; Jing, Y.; Tian, B.; Shi, X. Genome sequencing and analysis of *Bacillus velezensis* VJH504 reveal biocontrol mechanism against cucumber *Fusarium* wilt. *Front. Microbiol.* **2023**, *14*, 1279695. [[CrossRef](#)] [[PubMed](#)]
24. Schmiedeknecht, G.; Bochow, H.; Junge, H. Use of *Bacillus subtilis* as biocontrol agent. II. Biological control of potato diseases. *J. Plant Dis. Prot.* **1998**, *105*, 376–386.
25. Yao, A.V.; Bochow, H.; Karimov, S.; Boturov, U.; Sanginboy, S.; Sharipov, A.K. Effect of FZB 24 *Bacillus subtilis* as biofertilizer on cotton yields in field tests. *Arch. Phytopathol. Plant Prot.* **2006**, *39*, 323–328. [[CrossRef](#)]
26. Sylla, J.; Alsanius, B.W.; Krüger, E.; Reineke, A.; Strohmeier, S.; Wohanka, W. Leaf Microbiota of Strawberries as Affected by Biological Control Agents. *Phytopathology*® **2013**, *103*, 1001–1011. [[CrossRef](#)]
27. Talboys, P.J.; Owen, D.W.; Healey, J.R.; Withers, P.J.A.; Jones, D.L. Auxin secretion by *Bacillus amyloliquefaciens* FZB42 both stimulates root exudation and limits phosphorus uptake in *Triticum aestivum*. *BMC Plant Biol.* **2014**, *14*, 51. [[CrossRef](#)]
28. Chowdhury, S.P.; Dietel, K.; Rändler, M.; Schmid, M.; Junge, H.; Borriss, R.; Hartmann, A.; Grosch, R. Effects of *Bacillus amyloliquefaciens* FZB42 on Lettuce Growth and Health under Pathogen Pressure and Its Impact on the Rhizosphere Bacterial Community. *PLoS ONE* **2013**, *8*, e68818. [[CrossRef](#)]
29. Elanchezhian, K.; Keerthana, U.; Nagendran, K.; Prabhukarthikeyan, S.R.; Prabakar, K.; Raguchander, T.; Karthikeyan, G. Multifaceted benefits of *Bacillus amyloliquefaciens* strain FBZ24 in the management of wilt disease in tomato caused by *Fusarium oxysporum* f. sp. *lycopersici*. *Physiol. Mol. Plant Pathol.* **2018**, *103*, 92–101. [[CrossRef](#)]
30. Medeiros, C.A.; Bettiol, W. Multifaceted intervention of *Bacillus* spp. against salinity stress and *Fusarium* wilt in tomato. *J. Appl. Microbiol.* **2021**, *131*, 15095. [[CrossRef](#)]
31. Ma, S.; Wang, T.; Wang, Y. *Bacillus velezensis* K-9 as a Potential Biocontrol Agent for Managing Potato Scab. *Plant Dis.* **2023**, *107*, 3943–3951. [[CrossRef](#)] [[PubMed](#)]
32. Hardham, A.R.; Blackman, L.M. *Phytophthora cinnamomi*. *Mol. Plant Pathol.* **2018**, *19*, 260–285. [[CrossRef](#)] [[PubMed](#)]
33. Robold, A.V.; Hardham, A.R. During attachment *Phytophthora* spores secrete proteins containing thrombospondin type 1 repeats. *Curr. Genet.* **2005**, *47*, 307–315. [[CrossRef](#)] [[PubMed](#)]
34. Chang, H.-X.; Yendrek, C.R.; Caetano-Anolles, G.; Hartman, G.L. Genomic characterization of plant cell wall degrading enzymes and in silico analysis of xylanses and polygalacturonases of *Fusarium virguliforme*. *BMC Microbiol.* **2016**, *16*, 147. [[CrossRef](#)]
35. Xiong, W.; Guo, S.; Jousset, A.; Zhao, Q.; Wu, H.; Li, R.; Kowalchuk, G.A.; Shen, Q. Bio-fertilizer application induces soil suppressiveness against *Fusarium* wilt disease by reshaping the soil microbiome. *Soil Biol. Biochem.* **2017**, *114*, 238–247. [[CrossRef](#)]
36. Han, Q.; Ma, Q.; Chen, Y.; Tian, B.; Xu, L.; Bai, Y.; Chen, W.; Li, X. Variation in rhizosphere microbial communities and its association with the symbiotic efficiency of rhizobia in soybean. *ISME J.* **2020**, *14*, 1915–1928. [[CrossRef](#)]
37. Peterson, S.B.; Dunn, A.K.; Klimowicz, A.K.; Handelsman, J. Peptidoglycan from *Bacillus cereus* Mediates Commensalism with Rhizosphere Bacteria from the *Cytophaga-Flavobacterium* Group. *Appl. Environ. Microbiol.* **2006**, *72*, 5421–5427. [[CrossRef](#)]
38. Tao, C.; Li, R.; Xiong, W.; Shen, Z.; Liu, S.; Wang, B.; Ruan, Y.; Geisen, S.; Shen, Q.; Kowalchuk, G.A. Bio-organic fertilizers stimulate indigenous soil *Pseudomonas* populations to enhance plant disease suppression. *Microbiome* **2020**, *8*, 137. [[CrossRef](#)]
39. Sun, X.; Xu, Z.; Xie, J.; Hesselberg-Thomsen, V.; Tan, T.; Zheng, D.; Strube, M.L.; Dragoš, A.; Shen, Q.; Zhang, R.; et al. *Bacillus velezensis* stimulates resident rhizosphere *Pseudomonas stutzeri* for plant health through metabolic interactions. *ISME J.* **2022**, *16*, 774–787. [[CrossRef](#)]
40. Wang, W.; Portal-Gonzalez, N.; Wang, X.; Li, J.; Li, H.; Portieles, R.; Borrás-Hidalgo, O.; He, W.; Santos-Bermudez, R. Metabolome-driven microbiome assembly determining the health of ginger crop (*Zingiber officinale* L. Roscoe) against rhizome rot. *Microbiome* **2024**, *12*, 167. [[CrossRef](#)]
41. Jin, X.; Jia, H.; Ran, L.; Wu, F.; Liu, J.; Schlaeppli, K.; Dini-Andreote, F.; Wei, Z.; Zhou, X. Fusaric acid mediates the assembly of disease-suppressive rhizosphere microbiota via induced shifts in plant root exudates. *Nat. Commun.* **2024**, *15*, 5125. [[CrossRef](#)] [[PubMed](#)]
42. Matsumoto, H.; Fan, X.; Wang, Y.; Kusstatscher, P.; Duan, J.; Wu, S.; Chen, S.; Qiao, K.; Wang, Y.; Ma, B.; et al. Bacterial seed endophyte shapes disease resistance in rice. *Nat. Plants* **2021**, *7*, 60–72. [[CrossRef](#)] [[PubMed](#)]
43. Ping, X.; Khan, R.A.A.; Chen, S.; Jiao, Y.; Zhuang, X.; Jiang, L.; Song, L.; Yang, Y.; Zhao, J.; Li, Y.; et al. Deciphering the role of rhizosphere microbiota in modulating disease resistance in cabbage varieties. *Microbiome* **2024**, *12*, 160. [[CrossRef](#)]

44. Shaw, G.T.-W.; Liu, A.-C.; Weng, C.-Y.; Chen, Y.-C.; Chen, C.-Y.; Weng, F.C.-H.; Wang, D.; Chou, C.-Y. A network-based approach to deciphering a dynamic microbiome's response to a subtle perturbation. *Sci. Rep.* **2020**, *10*, 19530. [[CrossRef](#)]
45. Mougi, A.; Kondoh, M. Diversity of Interaction Types and Ecological Community Stability. *Science* **2012**, *337*, 349–351. [[CrossRef](#)]
46. Ma, Y.; Rajkumar, M.; Zhang, C.; Freitas, H. Beneficial role of bacterial endophytes in heavy metal phytoremediation. *J. Environ. Manag.* **2016**, *174*, 14–25. [[CrossRef](#)]
47. Santos-Medellín, C.; Edwards, J.; Liechty, Z.; Nguyen, B.; Sundaresan, V. Drought Stress Results in a Compartment-Specific Restructuring of the Rice Root-Associated Microbiomes. *mBio* **2017**, *8*, e00764-17. [[CrossRef](#)]
48. Yuan, Z.; Druzhinina, I.S.; Labbé, J.; Redman, R.; Qin, Y.; Rodriguez, R.; Zhang, C.; Tuskan, G.A.; Lin, F. Specialized Microbiome of a Halophyte and its Role in Helping Non-Host Plants to Withstand Salinity. *Sci. Rep.* **2016**, *6*, 32467. [[CrossRef](#)]
49. Hernandez, D.J.; David, A.S.; Menges, E.S.; Searcy, C.A.; Afkhami, M.E. Environmental stress destabilizes microbial networks. *ISME J.* **2021**, *15*, 1722–1734. [[CrossRef](#)]
50. Chen, E.; Chao, S.; Shi, B.; Liu, L.; Chen, M.; Zheng, Y.; Feng, X.; Wu, H. *Bacillus velezensis* ZN-S10 Reforms the Rhizosphere Microbial Community and Enhances Tomato Resistance to TPN. *Plants* **2023**, *12*, 3636. [[CrossRef](#)]

Disclaimer/Publisher's Note: The statements, opinions and data contained in all publications are solely those of the individual author(s) and contributor(s) and not of MDPI and/or the editor(s). MDPI and/or the editor(s) disclaim responsibility for any injury to people or property resulting from any ideas, methods, instructions or products referred to in the content.